



# Changing carbon-to-nitrogen ratios of organic-matter export under ocean acidification

Jan Taucher<sup>1</sup>✉, Tim Boxhammer<sup>1</sup>, Lennart T. Bach<sup>2</sup>, Allanah J. Paul<sup>1</sup>, Markus Schartau<sup>1</sup>, Paul Stange<sup>1</sup> and Ulf Riebesell<sup>1</sup>

**Ocean acidification (OA) will affect marine biotas from the organism to the ecosystem level. Yet, the consequences for the biological carbon pump and thereby the oceanic sink for atmospheric CO<sub>2</sub> are still unclear. Here we show that OA considerably alters the C/N ratio of organic-matter export (C/N<sub>export</sub>), a key factor determining efficiency of the biological pump. By synthesizing sediment-trap data from in situ mesocosm studies in different marine biomes, we find distinct but highly variable impacts of OA on C/N<sub>export</sub>, reaching up to a 20% increase/decrease under partial pressure of CO<sub>2</sub> ( $p_{CO_2}$ ) conditions projected for 2100. These changes are driven by  $p_{CO_2}$  effects on a variety of plankton taxa and corresponding shifts in food-web structure. Notably, our findings suggest a pivotal role of heterotrophic processes in controlling the response of C/N<sub>export</sub> to OA, thus contradicting the paradigm of primary producers as the principal driver of biogeochemical responses to ocean change.**

The downward flux of biogenic material from the surface to the deep ocean (biological pump) greatly enhances the ocean's capability to store carbon, thereby controlling atmospheric CO<sub>2</sub> on centennial to millennial timescales<sup>1,2</sup>. The carbon-to-nitrogen ratio of organic-matter export (C/N<sub>export</sub>) determines the amount of carbon that is transported from the euphotic zone to the ocean interior per unit nutrient, thereby controlling the efficiency of the biological pump as well as heterotrophic breakdown of organic matter and oxygen consumption in the deep ocean<sup>3</sup>. Thus, understanding how the environment influences the C/N ratio of organic matter and its spatial patterns in the global ocean has been one of the major objectives of biological oceanography for nearly a century<sup>4–6</sup>. Yet, little is known about how C/N<sub>export</sub> will respond to a changing ocean. Intensive research efforts over the past decade have demonstrated that ocean acidification (OA) can substantially influence marine biotas and the functioning of ecological communities<sup>7,8</sup>. However, potential impacts on biogeochemical cycling and the ocean carbon sink remain uncertain as most evidence is based on bottle experiments often insufficiently representing or neglecting ecological interactions and food-web dynamics in the ocean. Moreover, earlier work focused on C/N composition of primary producers and suspended biomass, not taking into account the changes in quality of sinking material, for example, due to zooplankton feeding and microbial degradation while being exported from the surface ocean<sup>9–11</sup>.

## OA on C/N of organic-matter export

Here we compile data on C/N composition of sinking particulate organic matter (POM) collected in sediment traps during five recent in situ OA experiments with entire plankton communities, ranging from bacteria to fish larvae<sup>12,13</sup>. The studies covered a wide latitudinal gradient ranging from the Arctic Ocean to the subtropical North Atlantic (Fig. 1a). Sinking POM was collected in sediment traps attached to the bottom of each mesocosm (Fig. 1b) and sampled every 1–2 days.

Impacts of OA on C/N<sub>export</sub> were quantified by calculating log-normalized response ratios ln(RR) as well as probability

densities for ambient conditions and CO<sub>2</sub> concentrations corresponding to end-of-century scenarios (representative concentration pathway (RCP) 6.0 to 8.5). To elucidate the underlying ecological drivers for changes in C/N<sub>export</sub>, we also quantified the partial pressure of CO<sub>2</sub> ( $p_{CO_2}$ ) responses of the variety of plankton taxa in the mesocosms and subsequently examined how changes in community composition were related to the observed patterns in C/N<sub>export</sub>.

Our analysis shows significant effects of OA on C/N<sub>export</sub> at all study sites. Observed effects in the different pelagic systems were highly variable, with ln(RR) ranging between +0.19 and -0.16, corresponding to a 20% increase or 17% decrease of carbon export per unit nitrogen (Fig. 2a). It should be noted that due to skewed data distributions, ln(RR) based on treatment averages indicated significant effects in only six out of eight cases, whereas the probability density estimates (that better account for non-normally distributed data) exhibited significant  $p_{CO_2}$ -related differences in all study regions and succession stages (Fig. 2b and Extended Data Fig. 1). This approach also revealed that elevated  $p_{CO_2}$  not only shifted mean C/N<sub>export</sub> but also altered the occurrence of extreme values. For example, in the Sweden study the probability of very high C/N ratios (>15) more than doubled under high  $p_{CO_2}$  (Fig. 2b).

In addition to the variability of CO<sub>2</sub> responses among study sites, we found a relatively high stochastic variability within the individual experiments, most likely originating from slight differences in the initial ecological conditions (Supplementary Information). Yet despite this underlying stochastic variability, OA triggered detectable shifts in C/N<sub>export</sub> in all experiments, irrespective of other environmental drivers such as nutrient availability and temperature, which strongly differed among study sites (Supplementary Fig. 2). Consequently, the observed sensitivity of C/N<sub>export</sub> to increasing  $p_{CO_2}$  seems to be a supra-regional and probably a global phenomenon.

## Food-web drivers behind C/N responses to high CO<sub>2</sub>

The substantial variability in observed C/N<sub>export</sub> responses is rather surprising and contrary to earlier conclusions. On the basis of findings from laboratory studies and the few existing CO<sub>2</sub> perturbation studies on entire plankton communities<sup>11,14</sup>, the common notion

<sup>1</sup>GEOMAR Helmholtz Centre for Ocean Research, Kiel, Germany. <sup>2</sup>Institute for Marine and Antarctic Studies, University of Tasmania, Hobart, Tasmania, Australia. ✉e-mail: [jtaucher@geomar.de](mailto:jtaucher@geomar.de)

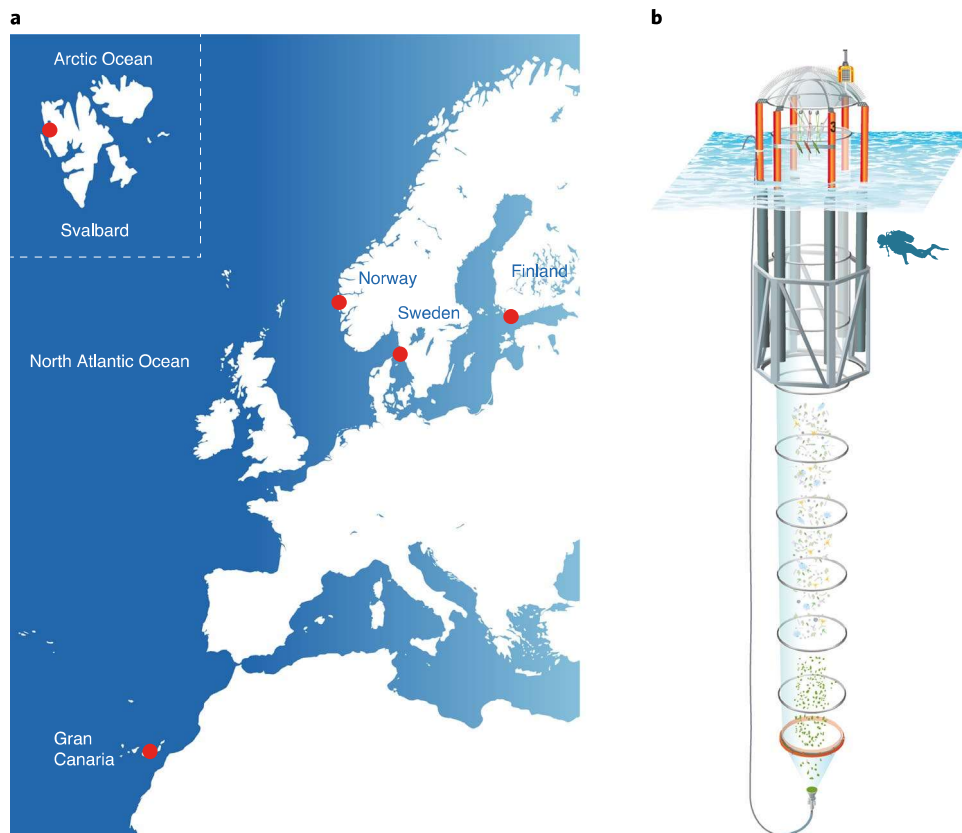


**Fig. 1 | Mesocosm experiment locations and design.** **a**, Locations of large-volume in situ mesocosm experiments. **b**, Schematic drawing of a pelagic mesocosm enclosing the natural plankton community and collecting sinking organic matter in a full-diameter sediment trap at the bottom (15–25 m water depth, depending on study site). Illustration by Rita Erven (GEOMAR), reprinted with permission from the AGU.

emerged that OA would lead to a rather uniform increase in C/N, presuming that this response is driven primarily by physiological effects on phytoplankton (for example, CO<sub>2</sub> fertilization of photosynthesis)<sup>15–17</sup>. Accordingly, one would expect that OA responses of C/N<sub>export</sub> can be explained by pCO<sub>2</sub> responses of the dominant primary producers.

Our analysis reveals highly variable effects of elevated pCO<sub>2</sub> on phytoplankton. Depending on study region and nutrient conditions, we found considerable differences in the phytoplankton taxa being affected, as well as in the direction and magnitude of pCO<sub>2</sub> effects (Fig. 3a). However, identifying how OA effects on individual taxa contributed to shifts in C/N<sub>export</sub> is challenging, due mainly to the inherent variability of C/N of the various taxa in natural phytoplankton assemblages.

Only in very few situations, when a single taxon dominated biomass, did we find indications that physiological pCO<sub>2</sub> effects on the dominant primary producers were strong enough to leave an imprint on the C/N of exported organic matter (Supplementary Tables 2 and 3, for example, Sweden, nutrient-limited). However, there was no consistent pattern in the pCO<sub>2</sub> responses of the various phytoplankton taxa and their correlations with C/N<sub>export</sub>, that could explain the variability in magnitude or even direction of observed OA effects on C/N<sub>export</sub> across the various study regions and succession stages (Fig. 3b). For example, in the Svalbard study, all pCO<sub>2</sub> responses detected for the various phytoplankton taxa were positive during both experimental phases (Fig. 3a); however, pCO<sub>2</sub> effects on C/N<sub>export</sub> occurred in contrasting directions (Fig. 2). This indicates the predominance of other processes within the plankton community rather than phytoplankton physiology in driving the response of C/N<sub>export</sub>.

We found strong evidence for a key role of heterotrophic processes in shaping the C/N ratio of organic-matter export and its response to elevated pCO<sub>2</sub>. A comparison between C/N ratios of sediment-trap material (C/N<sub>export</sub>) with those of suspended POM (C/N<sub>water</sub>) revealed a marked increase in C/N during sinking in all experiments (Fig. 4a–h). This pattern probably reflects consumption and degradation of sinking particles by zooplankton and heterotrophic bacteria, which is usually associated with preferential remineralization of N over C and thereby increasing C/N in sinking particles<sup>18,19</sup>. Notably, we identified a significant influence of pCO<sub>2</sub> on this change in C/N during sinking in the majority of studies ( $\Delta C/N_{sink}$  given as  $\frac{C/N_{export}}{C/N_{water}}$ , Fig. 4i–p). Moreover, five out of six situations for which we observed OA impacts on C/N<sub>export</sub> coincided with corresponding pCO<sub>2</sub> effects on preferential N remineralization as defined by  $\Delta C/N_{sink}$  (Figs. 2 and 4). The influence of pCO<sub>2</sub> on the degradation of sinking material may also explain why our findings are partly contrasting to earlier studies, which examined OA impacts on C/N stoichiometry without differentiating between suspended and sinking organic matter as done here.

Differences in the magnitude of  $\Delta C/N_{sink}$  among experiments, as well as its variable response to elevated pCO<sub>2</sub>, probably reflect differences in food-web structure among study sites and trophic states. This variability may be related to (1) the quality and lability of produced organic material and/or (2) the abundance and activity of heterotrophic consumers. Indeed, our analysis disclosed a considerable number of pCO<sub>2</sub> effects on meso- and microzooplankton, as well as bacteria in the different experiments (Fig. 3a).

Zooplankton communities in most study regions were dominated by copepods, which displayed variable responses to pCO<sub>2</sub> and correlations with C/N<sub>export</sub> (Fig. 3). Most earlier work suggested a

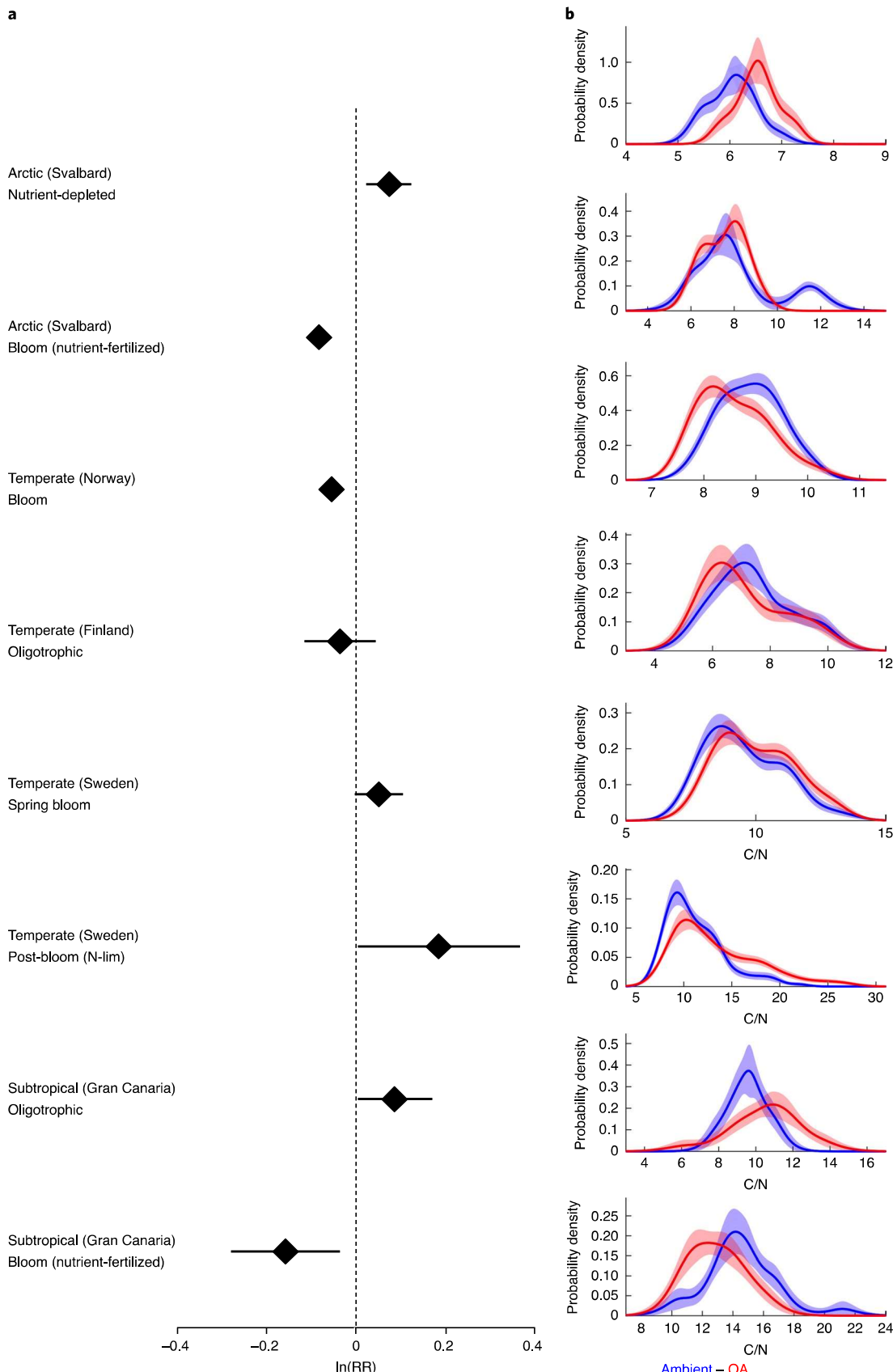


**Fig. 2 | Impact of simulated OA on C/N ratios of sinking particulate matter in the different in situ mesocosm studies.** **a**, Mean effect size calculated as the log of the response ratio  $\ln(\text{RR})$  of the treatment average, including 95% confidence intervals. **b**, Probability density estimates of actual C/N ratios under ambient conditions (blue) and OA (red) with shaded areas denoting standard deviation. Note different scales of x-axes due to large variations in baseline C/N among study regions. Non-overlapping density estimates indicate statistically significant differences in probability distributions of C/N. N-lim, nutrient limitation.

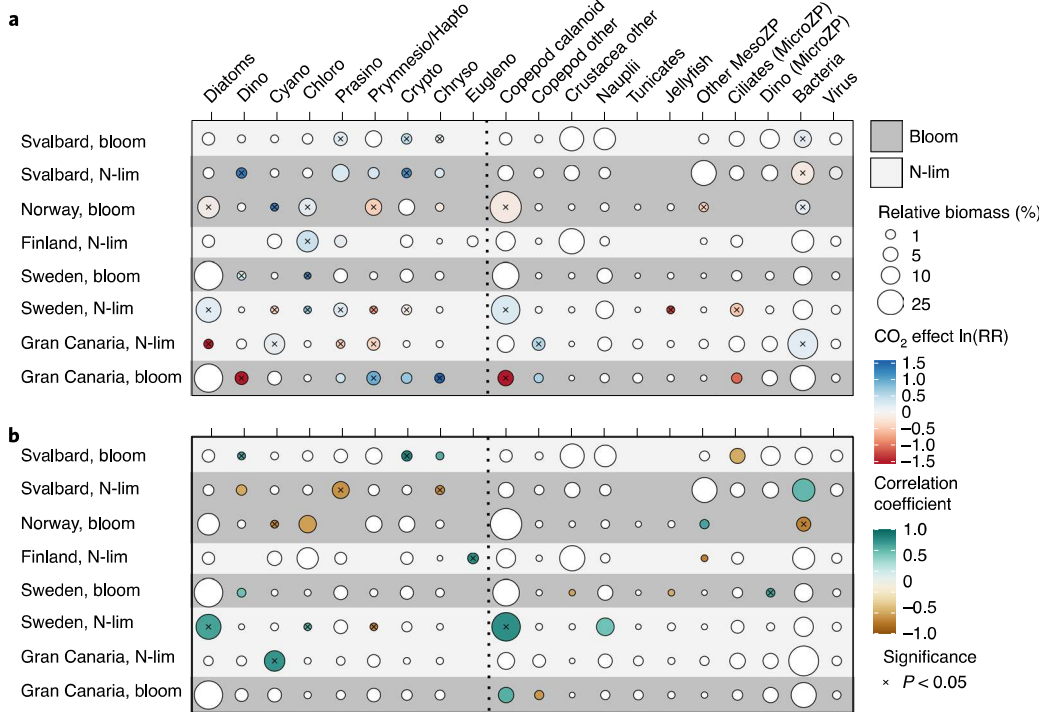


**Fig. 3 | The role of plankton communities in shaping OA impacts on the C/N ratio of organic-matter export.** **a**, Responses of different plankton taxa to simulated OA. Heatmap colours denote effect size, given as the log of the response ratio ln(RR) of the treatment average. Circle size denotes relative biomass of the various plankton groups within studies (averaged over all CO<sub>2</sub> treatments) to illustrate which groups may have had a potentially large influence on C/N of sinking organic matter. **b**, Correlation between biomass of plankton taxa and the C/N ratio of organic-matter export. Heatmap colours indicate the Pearson correlation coefficient. For both **a** and **b**, calculations are based on temporally averaged data from individual mesocosms and succession phase for each experiment (see Methods for details). The vertical dotted line separates autotrophic taxa (left) from heterotrophic taxa (right). Grey shading highlights the trophic state of the ecosystem; that is, bloom conditions (dark) or nutrient limitation (light). Crosses denote statistically significant effects ( $P < 0.05$ ), but trends with a higher significance threshold ( $P < 0.1$ ) are also coloured. See Supplementary Table 5 for source data.

minor role of direct (physiological) OA impacts on copepods, compared with indirect CO<sub>2</sub> effects mediated through changes in food quantity and quality<sup>20,21</sup>. However, these previous studies also found that CO<sub>2</sub>-related changes in the biochemical composition of phytoplankton, which are not necessarily visible in their C/N/P stoichiometry, can substantially affect the performance of mesozooplankton grazers. Accordingly, we consider it likely that observed zooplankton responses were mediated by  $p_{\text{CO}_2}$  effects on phytoplankton and corresponding changes in prey quantity and/or quality, which in turn altered feeding interactions and the degradation of sinking organic matter (see Supplementary Table 3 for details, for example, Sweden, nutrient-limited; Gran Canaria, bloom). Heterotrophic bacteria are another key player in organic-matter turnover. They constituted a remarkable portion of overall plankton biomass (between 10% and 40% depending on study site) and displayed variable responses to high  $p_{\text{CO}_2}$  (Fig. 3). Besides standing stocks, activity of bacterial hydrolytic enzymes was measured in two of the mesocosm experiments (Svalbard and Norway) and was considerably enhanced under OA conditions in both studies<sup>22,23</sup> (Supplementary Table 3). Taken together, all cases in which OA affected  $\Delta \text{C}/\text{N}_{\text{sink}}$  coincided with  $p_{\text{CO}_2}$  effects on zooplankton and/or bacteria (Figs. 3 and 4), indicating that organic-matter turnover and preferential N remineralization by heterotrophic organisms played an important role in shaping the response of  $\text{C}/\text{N}_{\text{export}}$  to OA.

It should be noted that the interpretations outlined in the preceding are based mainly on comparisons between C/N data and biomass of different plankton groups, thus not allowing us to mechanistically demonstrate or even quantify the influence of specific taxa on C/N. This would have required further-reaching analysis

such as sorting of various phytoplankton taxa and measurement of their specific C/N (for example, by cell-sorting flow cytometry), determining the composition of sinking detritus (for example, proportions of phytodetritus, faecal pellets and so on), as well as incubating organic material with individual heterotrophic groups to assess how they alter its C/N.

Nevertheless, our findings are a major step forward as they challenge the prevailing autotroph-centric paradigm, which considers phytoplankton as the primary driver of C/N ratios and their response to ocean change<sup>14–16</sup>. Considering the multitude of  $p_{\text{CO}_2}$  effects on primary producers, zooplankton, bacteria and viruses, it is highly likely that they all contributed to the observed changes in  $\text{C}/\text{N}_{\text{export}}$ . Yet, from a synoptic view, there was no consistent overarching pattern in the  $p_{\text{CO}_2}$  responses of the various plankton taxa across all experiments from which shifts in  $\text{C}/\text{N}_{\text{export}}$  could be unambiguously inferred or predicted. One reason is that relative contributions of individual plankton taxa to overall biomass varied substantially between study regions and even among succession stages during a given experiment (Fig. 3). It is therefore likely that food-web structure and pathways of organic matter, from production over degradation to export, differed markedly as well. In a broader sense,  $\text{C}/\text{N}_{\text{export}}$  reflects a multitude of processes within an ecological network, which in their entirety leave an imprint on the biochemical and elemental composition of organic particles. Accordingly, direction and magnitude of OA impacts on  $\text{C}/\text{N}_{\text{export}}$  reflect the sum of  $p_{\text{CO}_2}$  sensitivities of the individual nodes (that is, species) in the plankton network. This holistic view also explains why  $p_{\text{CO}_2}$  effects on individual taxa are not sufficient to predict how  $\text{C}/\text{N}_{\text{export}}$  will respond to OA.

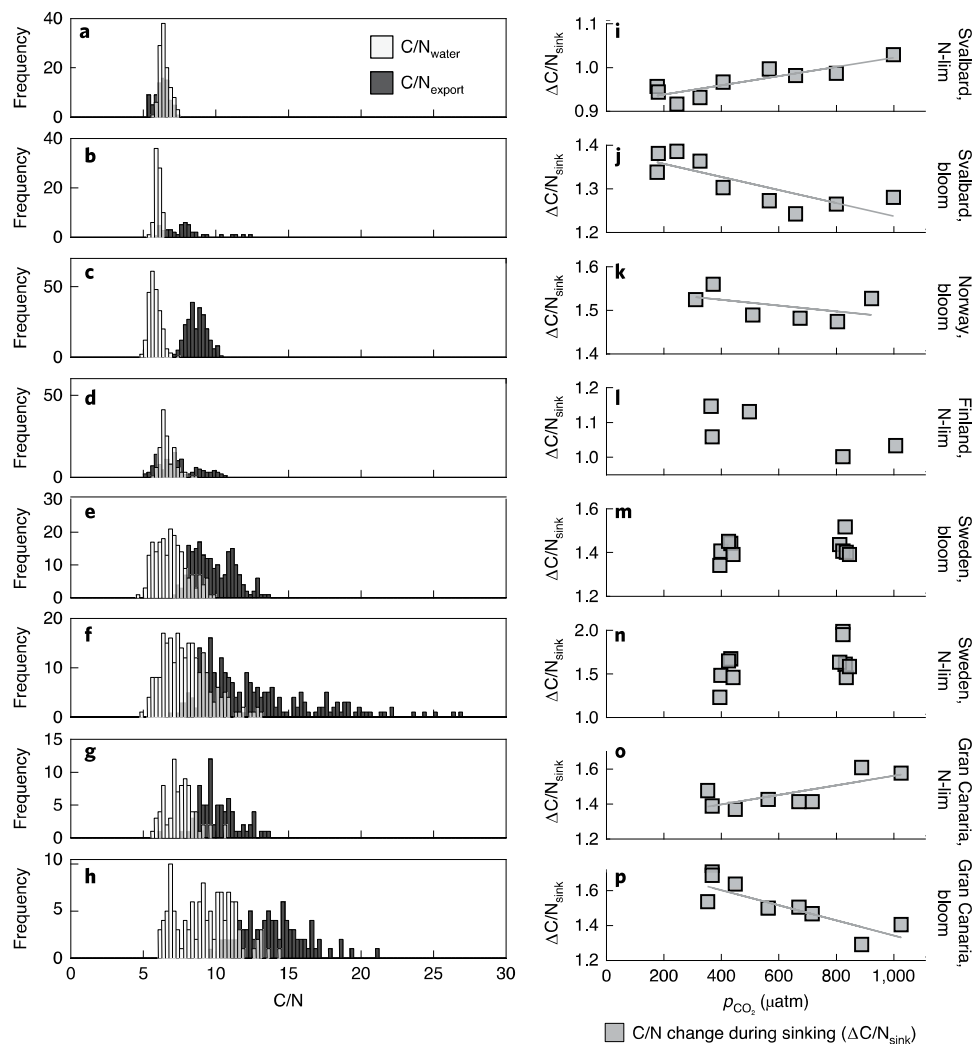


**Fig. 4 | Change in C/N of sinking particles and its response to OA.** **a–h**, Difference between C/N ratios of sinking particles (dark grey) compared with those of material suspended in the water column (light grey): Svalbard, N-lim (**a**); Svalbard, bloom (**b**); Norway, bloom (**c**); Finland, N-lim (**d**); Sweden, bloom (**e**); Sweden, N-lim (**f**); Gran Canaria, N-lim (**g**); and Gran Canaria, bloom (**h**). Note that C/N ratios usually increased notably during sinking, probably reflecting preferential remineralization of nitrogen by heterotrophic consumers (zooplankton, bacteria). Histograms include all available data from the individual studies, independent of  $p_{CO_2}$  treatment (that is, entire time series of all mesocosms). Scaling of x-axes is kept identical to illustrate the large variability in C/N among study regions. **i–p**, Influence of OA on the change in C/N ratios of organic material during sinking ( $\Delta C/N_{sink}$ ), given as the fraction of C/N of sediment-trap material and particulate matter suspended in the water column ( $\frac{C/N_{export}}{C/N_{water}}$ ): Svalbard, N-lim (**i**); Svalbard, bloom (**j**); Norway, bloom (**k**); Finland, N-lim (**l**); Sweden, bloom (**m**); Sweden, N-lim (**n**); Gran Canaria, N-lim (**o**); and Gran Canaria, bloom (**p**). A value of 1 would indicate that no change in C/N occurred during sinking. In the majority of cases (five out of eight), we found a distinct influence of increasing  $p_{CO_2}$  on the change in C/N during sinking (indicated by a grey line when regression analysis was significant with  $P < 0.05$ ), indicating that organic-matter turnover and preferential remineralization of nitrogen by heterotrophic consumers were affected by OA. Note that only mesocosms with  $p_{CO_2}$  up to ~1,000 μatm were considered for this analysis, consistent with the analysis shown in Figs. 2 and 3.

At the same time, we found indications for a general pattern linking OA impacts on  $C/N_{export}$  to nutrient availability and the trophic state of the plankton communities. Most positive responses of  $C/N_{export}$  to simulated OA occurred under nutrient-limited conditions, whereas bloom situations rather led to lower  $C/N_{export}$  under high  $p_{CO_2}$  (Fig. 2). As outlined in the preceding, our findings suggest that heterotrophic processes were crucial in determining  $C/N_{export}$  in the majority of our studies. Consequently, we hypothesize that the variable CO<sub>2</sub> response pattern of  $C/N_{export}$  is related to varying influences of zooplankton and bacteria on the degradation of organic matter during oligotrophic conditions and phytoplankton blooms, as well as variable sensitivities of these key groups to elevated  $p_{CO_2}$  under different trophic conditions.

### Biogeochemical cycles under OA

Our study provides evidence that OA could induce marked shifts in C/N ratios of organic-matter export over the coming centuries. Depending on the direction of the  $p_{CO_2}$  response, such changes in carbon export efficiency (defined as the amount of carbon exported for a given nutrient input) would dampen or amplify the projected weakening of the biological pump in a warmer and more stratified ocean<sup>24,25</sup>. In fact, earlier modelling efforts found changes in C/N to drive moderate feedbacks on ocean carbon sequestration, corresponding to 15–30 μatm atmospheric  $p_{CO_2}$  until year 2100<sup>17,26,27</sup>. In addition, studies on glacial–interglacial cycles indicate that the impact of elemental stoichiometry on the strength of the ocean carbon sink may become increasingly relevant on longer timescales<sup>28,29</sup>.

On regional scales, changes in C/N<sub>export</sub> could alter microbial oxygen demand at mesopelagic depths, thereby severely affecting the expansion of oxygen minimum zones in these high-export regions<sup>27</sup>. Our findings demonstrate that looking beyond physiological CO<sub>2</sub> effects on individual taxa and considering ecological interactions and organic-matter fluxes within plankton communities is essential for predicting large-scale patterns of C/N stoichiometry and their consequences for the biological pump in the future ocean.

## Online content

Any methods, additional references, Nature Research reporting summaries, source data, extended data, supplementary information, acknowledgements, peer review information; details of author contributions and competing interests; and statements of data and code availability are available at <https://doi.org/10.1038/s41558-020-00915-5>.

Received: 5 February 2019; Accepted: 24 August 2020;

Published online: 19 October 2020

## References

- Kwon, E. Y., Primeau, F. & Sarmiento, J. L. The impact of remineralization depth on the air-sea carbon balance. *Nat. Geosci.* **2**, 630–635 (2009).
- Volk, T. & Hoffert, M. I. in *The Carbon Cycle and Atmospheric CO<sub>2</sub>: Natural Variations Archean to Present* Vol. 32 (eds Sundquist, E. T. & Broeker, W. S.) 99–110 (American Geophysical Union, 1985).
- Passow, U. & Carlson, C. A. The biological pump in a high CO<sub>2</sub> world. *Mar. Ecol. Prog. Ser.* **470**, 249–271 (2012).
- Martiny, A. C. et al. Strong latitudinal patterns in the elemental ratios of marine plankton and organic matter. *Nat. Geosci.* **6**, 279–283 (2013).
- DeVries, T. New directions for ocean nutrients. *Nat. Geosci.* **11**, 15–16 (2018).
- Redfield, A. in *James Johnstone Memorial Volume* (ed. Daniel, R. J.) 177–192 (University Press of Liverpool, 1934).
- Kroeker, K. J., Kordas, R. L., Crim, R. N. & Singh, G. G. Meta-analysis reveals negative yet variable effects of ocean acidification on marine organisms. *Ecol. Lett.* **13**, 1419–1434 (2010).
- Riebesell, U. & Tortell, P. D. in *Ocean Acidification* (eds Gattuso, J. P. & Hansson, L.) 99–121 (Oxford Univ. Press, 2011).
- Boyd, P. W. & Newton, P. P. Does planktonic community structure determine downward particulate organic carbon flux in different oceanic provinces? *Deep Sea Res. I* **46**, 63–91 (1999).
- Stange, P. et al. Ocean acidification-induced restructuring of the plankton food web can influence the degradation of sinking particles. *Front. Mar. Sci.* <https://doi.org/10.3389/fmars.2018.00140> (2018).
- Engel, A. et al. Impact of CO<sub>2</sub> enrichment on organic matter dynamics during nutrient induced coastal phytoplankton blooms. *J. Plankton Res.* **36**, 641–657 (2014).
- Riebesell, U. et al. Technical note: a mobile sea-going mesocosm system—new opportunities for ocean change research. *Biogeosciences* **10**, 1835–1847 (2013).
- Sswat, M. et al. Food web changes under ocean acidification promote herring larvae survival. *Nat. Ecol. Evol.* <https://doi.org/10.1038/s41559-018-0514-6> (2018).
- Riebesell, U. et al. Enhanced biological carbon consumption in a high CO<sub>2</sub> ocean. *Nature* **450**, 545–548 (2007).
- Finkel, Z. V. et al. Phytoplankton in a changing world: cell size and elemental stoichiometry. *J. Plankton Res.* **32**, 119–137 (2010).
- van de Waal, D. B., Verschoor, A. M., Verspagen, J. M. H., van Donk, E. & Huisman, J. Climate-driven changes in the ecological stoichiometry of aquatic ecosystems. *Front. Ecol. Environ.* **8**, 145–152 (2010).
- Tagliabue, A., Bopp, L. & Gehlen, M. The response of marine carbon and nutrient cycles to ocean acidification: large uncertainties related to phytoplankton physiological assumptions. *Glob. Biogeochem. Cycle* <https://doi.org/10.1029/2010gb003929> (2011).
- Thomas, H., Ittekot, V., Osterroth, C. & Schneider, B. Preferential recycling of nutrients—the ocean's way to increase new production and to pass nutrient limitation? *Limnol. Oceanogr.* **44**, 1999–2004 (1999).
- Schneider, B., Schlitzer, R., Fischer, G. & Nothig, E. M. Depth-dependent elemental compositions of particulate organic matter (POM) in the ocean. *Glob. Biogeochem. Cycle* <https://doi.org/10.1029/2002gb001871> (2003).
- Cripps, G., Flynn, K. J. & Lindeque, P. K. Ocean acidification affects the phyto-zoo plankton trophic transfer efficiency. *PLoS ONE* <https://doi.org/10.1371/journal.pone.0151739> (2016).
- Thor, P. & Oliva, E. O. Ocean acidification elicits different energetic responses in an Arctic and a boreal population of the copepod *Pseudocalanus acuspes*. *Mar. Biol.* **162**, 799–807 (2015).
- Endres, S., Galgani, L., Riebesell, U., Schulz, K. G. & Engel, A. Stimulated bacterial growth under elevated pCO<sub>2</sub>: results from an off-shore mesocosm study. *PLoS ONE* **9**, e99228 (2014).
- Piontek, J. et al. Response of bacterioplankton activity in an Arctic fjord system to elevated pCO<sub>2</sub>: results from a mesocosm perturbation study. *Biogeosciences* **10**, 297–314 (2013).
- Bopp, L. et al. Multiple stressors of ocean ecosystems in the 21st century: projections with CMIP5 models. *Biogeosciences* **10**, 6225–6245 (2013).
- Taucher, J. & Oschlies, A. Can we predict the direction of marine primary production change under global warming? *Geophys. Res. Lett.* <https://doi.org/10.1029/2010gl045934> (2011).
- Schneider, B., Engel, A. & Schlitzer, R. Effects of depth- and CO<sub>2</sub>-dependent C:N ratios of particulate organic matter (POM) on the marine carbon cycle. *Glob. Biogeochem. Cycle* <https://doi.org/10.1029/2003gb002184> (2004).
- Oschlies, A., Schulz, K. G., Riebesell, U. & Schmittner, A. Simulated 21st century's increase in oceanic suboxia by CO<sub>2</sub>-enhanced biotic carbon export. *Glob. Biogeochem. Cycle* <https://doi.org/10.1029/2007gb003147> (2008).
- Broecker, W. S. & Henderson, G. M. The sequence of events surrounding Termination II and their implications for the cause of glacial-interglacial CO<sub>2</sub> changes. *Paleoceanography* **13**, 352–364 (1998).
- Broecker, W. S. Ocean chemistry during glacial time. *Geochim. Cosmochim. Acta* **46**, 1689–1705 (1982).

**Publisher's note** Springer Nature remains neutral with regard to jurisdictional claims in published maps and institutional affiliations.

© The Author(s), under exclusive licence to Springer Nature Limited 2020

## Methods

**Mesocosm experiments.** Between 2010 and 2014, we conducted five experiments with the Kiel Off-Shore Mesocosms for Future Ocean Simulations at different locations covering a large latitudinal gradient and diverse oceanic environments/ecosystems (Supplementary Table 1). The mesocosms enclosed the natural plankton communities in the respective study locations under close-to-natural conditions. Simulation of OA scenarios was achieved by adding filtered, CO<sub>2</sub>-saturated seawater equally distributed into the mesocosms as described by Riebesell and colleagues<sup>12</sup>. CO<sub>2</sub> enrichment was carried out at the beginning of the experiment, and usually several more times throughout the experiments, to maintain carbonate chemistry within target levels. Ranges of  $p_{CO_2}$ , as well as an overview of some technical details and environmental conditions during the experiments are summarized in Supplementary Table 1. Further details on experimental set-ups are thoroughly described in the specific overview papers for the individual studies (see Supplementary Table 1 for references).

**Definition of succession stages and experimental phases.** As the duration of the mesocosm experiments ranged between 1 and 4 months (Supplementary Table 1), some studies covered large temporal changes in environmental conditions and plankton succession. To account for the temporal differences in plankton community composition, element cycling and the C/N ratio of organic-matter export, it was necessary to divide some of the respective experiments into separate phases for analysis of  $p_{CO_2}$  effects.

For the study in the Arctic (Svalbard), we distinguish between an initial early-summer post-bloom phase ('Svalbard, nutrient-limited') with relatively low chlorophyll *a* (Chl *a*) concentrations (days 1–13) and a plankton bloom that developed in response to nutrient fertilization (days 13–22), displaying elevated Chl *a* and higher fluxes of organic-matter export ('Svalbard, bloom'). A subsequent bloom was still in progress when the experiment had finished and was not considered in the present analysis, as the material from this event did not reach the sediment traps (see 'Assessing the influence of plankton communities on C/N of organic-matter export').

The Norway study was characterized by late-spring bloom conditions throughout the entire experiment period. A first bloom developed from nutrients available at the start of the experiment and was followed by a second bloom after addition of inorganic nutrients two weeks later. However, since community composition and biogeochemical patterns remained relatively constant during the 5-week study, it was not necessary to divide the experiment into separate phases. Thus, we integrated data covering the entire experimental period into our analysis framework ('Norway, bloom').

Similarly, we did not divide data from the Finland experiment into separate phases, as the study covered a prolonged period of typical summer conditions with persistently low nutrient and chlorophyll concentrations ('Finland, nutrient-limited').

The Sweden study was the longest experiment, lasting for almost 4 months and covering the entire natural spring bloom succession. We divided the experiment into the initial spring bloom ('Sweden, bloom'), which was characterized by rapid uptake of inorganic nutrients (that were naturally present in the enclosed water bodies), the rapid development of a diatom bloom (dominated by small species) and a strong temporal decoupling of phytoplankton growth and zooplankton grazing (days 0–41), and the post-bloom stage ('Sweden, nutrient-limited') after nutrient depletion on day 37, when phytoplankton biomass was dominated by the large diatom *Coscinodiscus concinnus*, and micro- and mesozooplankton populations reached their peak biomass (days 41–87).

Finally, the experiment off the coast of Gran Canaria started with a period of oligotrophic conditions ('Gran Canaria, nutrient-limited') typical for subtropical oceans (days 1–23). Afterwards, we added deep water from >600 m depth to the mesocosms to simulate a natural upwelling event, which regularly occurs due to eddies in the study region. This triggered the development of a plankton bloom ('Gran Canaria, bloom') and an extended period of enhanced organic-matter export (days 25–55).

**Sediment-trap sampling and C/N measurements.** Sinking particulate material was obtained from sediment traps attached to the bottom of the mesocosms, thereby collecting the entire material sinking down in the enclosed water column<sup>12</sup>. Sample collection and processing of the sediment-trap material was conducted every 1 or 2 days, covering the entire duration of the various experiments (ranging between 30 and 107 days) and following the procedure described by Boxhammer et al.<sup>30</sup>.

In study locations where calcifying plankton occurred (Svalbard 2010, Norway 2011, Gran Canaria 2014), we distinguished between total particulate carbon (TPC) and particulate organic carbon (POC) by acidifying subsamples with 1 M HCl (for 1 h) before measurement to remove particulate inorganic carbon (PIC). For the other study sites, only TPC samples were measured and assumed to be composed entirely of POC (Finland 2012, Sweden 2013). Concentrations of TPC, POC and PON were determined using an elemental CN analyser (EuroEA) following Sharp<sup>31</sup>. For the analysis presented here, we used POC/PON data when available, and TPC/PON when measurements of POC were not performed, that is, when the contribution of PIC to TPC was negligible.

**Data analysis and assessment of CO<sub>2</sub> effects on C/N<sub>export</sub>.** As described in the preceding, the experimental design and the range of CO<sub>2</sub> treatments varied among the different experiments (Supplementary Table 1). The calculation of effect size with log response ratios is designed to compare average values of specific (and replicated) treatments. Thus, it was necessary to assign several mesocosms with different CO<sub>2</sub> concentrations into groups, in cases a gradient design was applied in the respective experiment.

Therefore, we pooled mesocosms with temporally averaged  $p_{CO_2}$  values between ~700 and 1,000  $\mu\text{atm}$  ('OA treatment'), corresponding to CO<sub>2</sub> concentrations as expected for the end of this century in the range of RCP scenarios 6.0 and 8.5 (ref. <sup>32</sup>). A similar procedure was applied for the control treatment, which included the mesocosms left at ambient CO<sub>2</sub> and, in cases of regression set-up, those with a CO<sub>2</sub> elevated by a maximum of 100  $\mu\text{atm}$  relative to ambient. This was necessary to acquire large enough sample numbers for obtaining reliable confidence intervals for the effect sizes. Effect sizes were calculated as log-transformed response ratios ln(RR) of the treatment mean, an approach commonly used in meta-analysis<sup>33</sup>:

$$\ln(\text{RR}) = \ln(X_{\text{OA}}) - \ln(X_{\text{control}})$$

where  $X$  is the arithmetic mean of C/N<sub>export</sub> ratios in the CO<sub>2</sub>-treated (OA) and control mesocosms (Supplementary Table 1). Effect sizes <0 denote a negative effect of OA, and effect sizes >0 denote that the effect was positive. Effects are considered statistically significant when confidence intervals, calculated from pooled standard deviations of both treatments, do not overlap with zero<sup>33</sup>.

In meta-analysis, these calculations are usually conducted to compute an 'overall effect' across all studies. We did not calculate and present such an overall effect in the present study. The main reason is that this approach assumes that variability between study results from 'random effects', for example, differences in data quality or random variation (observational noise). However, on the basis of our data analysis and ecological interpretation, we are convinced that the observed variability in C/N responses to OA was attributable to differences in the interplay between plankton community composition and elemental cycling rather than observational noise. Therefore, we show effect sizes of the individual studies to highlight the variability of the response, instead of calculating a—probably misleading—overall effect.

In addition to (parametric) log-transformed effect sizes, we computed probability densities of C/N ratios on the basis of kernel density estimation, which is a non-parametric method that better accounts for data with skewed or multimodal distributions. Another advantage of this approach is that it does not require the calculation of temporal means. Instead, the entire data time series of individual mesocosms can be incorporated into the data analysis, thus retaining information about temporal variability such as peaks and troughs in the datasets. We used C/N data from the same CO<sub>2</sub> treatments as used for calculating effect size as described in the preceding. In addition, we applied a bootstrapping approach to resample raw data (with replacement, sample size =  $n$  of observations, 1,000 permutations) and thereby estimate confidence intervals of the density estimates, following the approach described by Schartau et al.<sup>34</sup>. Statistically significant differences among treatments are assumed if confidence intervals of the density distributions do not overlap.

**Variability of C/N responses to OA among study sites and within experiments.** Analysis of the various mesocosm datasets following the procedure described in the preceding revealed a considerable variability of CO<sub>2</sub> effects on C/N, both between different experiments and within individual experiments.

Regarding the variability between experiments, our analyses indicated that this is driven by true differences in ecological and biogeochemical processes among study sites. Since plankton communities differed substantially among study sites, it is highly likely that variations in C/N responses among experiments originate from differences in plankton community composition. In addition to this, however, it should be noted that we also observed a relatively large degree of stochastic variability within the individual studies (Supplementary Table 2). The most likely explanation for this within-experiment variability is that the plankton communities enclosed in the beginning of the experiments already differed slightly due to plankton patchiness: mesocosm field study sites usually measured 150 × 150 m, so it is likely that some (usually small) degree of ecological variability within this area occurred at the time when the experiments were started, thus enclosing slightly different communities in the individual mesocosms. It can be assumed that these subtle differences in food-web structure became larger over the succession of several weeks to months (that is, the duration of the mesocosm experiments).

Clearly, statistically detecting (or excluding) CO<sub>2</sub> effects on C/N ratios in the presence of this underlying variation is challenging, particularly with the limited number of mesocosms in these large-scale field experiments. This is also one of the reasons we performed two independent techniques with individual strengths and weaknesses (classical meta-analysis and probability densities, see section titled 'Data analysis and assessment if CO<sub>2</sub> effects on C/N<sub>export</sub>') for the assessment and quantification of CO<sub>2</sub> effects. At the same time, the fact that we detected statistically significant CO<sub>2</sub> effects on plankton communities and C/N stoichiometry despite the relatively large stochastic variability gives us confidence that the identified OA impacts are robust and truly a widespread phenomenon, for

example, not occurring only under very specific conditions or when communities have a certain composition.

**Plankton sampling and biomass estimates of individual taxa.** Water samples for phytoplankton, microzooplankton, bacteria (that is, heterotrophic bacterioplankton), viruses and suspended POM were obtained with depth-integrating water samplers (IWS, HYDRO-BIOS), which gently collect a volume of 5 litres uniformly distributed over the depth of the mesocosms. The sampling interval was every 1 or 2 days, depending on the experiment. Mesozooplankton was sampled with Apstein nets (55 µm mesh size, 0.17 m diameter opening) in 8-day intervals.

Subsamples for Chl *a* and other phytoplankton pigments were collected onto glass fibre filters (GF/F Whatman, pore size: 0.7 µm) and analysed by reverse-phase high-performance liquid chromatography. Contributions of individual phytoplankton groups to total Chl *a* were then estimated using the CHEMOTAX software, which classifies phytoplankton on the basis of taxon-specific pigment ratios<sup>35</sup>.

Microzooplankton samples were usually analysed in a light microscope in 6- to 8-day intervals using the Utermöhl technique<sup>36</sup>. In the scope of this study, we distinguished between ciliates and heterotrophic dinoflagellates.

Mesozooplankton abundances were acquired from counting net samples on a stereomicroscope, including classification until the species level, or the lowest possible taxonomical level in cases where certain determination of species could not be achieved. For the analysis in the present study, we classified counted organisms into seven taxonomic groups: calanoid copepods, other (non-calanoid) copepods, other crustaceans, nauplii, tunicates, jellyfish (including hydrozoans and cnidophores) and other mesozooplankton.

Concentrations of bacteria and viruses were determined by flow cytometry (FACSCalibur or Accuri C6). Therefore, samples were diluted with Tris-EDTA buffer and stained with the green fluorescent nucleic acid-specific dye SYBR-Green I.

Abundances of the various plankton taxa were converted to biomass by applying the respective conversion factors from published literature (Supplementary Table 4).

Besides plankton, we also collected samples for particulate matter suspended in the water column. Samples were filtered onto pre-combusted GF/F glass fibre filters (450 °C for 6 h), and concentrations of carbon and nitrogen were measured on an elemental CN analyser (EuroEA) following Sharp<sup>31</sup>. Analogous to sediment-trap material, we distinguished between TPC and POC by fuming some of the replicate filters with hydrochloric acid (37 %) for 2 h before measurement<sup>37</sup> to remove PIC. For the C/N ratios of suspended particulate matter presented here, we used POC/PON data when available and TPC/PON when measurements of POC were not performed, that is, when the contribution of PIC to TPC was practically zero.

**Quantifying OA impacts on plankton communities.** To examine effects of simulated OA on plankton communities, we applied linear regression analysis to detect significant effects of increasing  $p_{CO_2}$  on the biomass of different plankton taxa. Therefore, we used temporally averaged data for individual mesocosms and respective experimental phases for each study site. Furthermore, we used all mesocosms from the individual studies to increase statistical power, that is, not only the ones pooled into the 'control' and 'OA' ranges of  $p_{CO_2}$  as done for the calculation of effect sizes (Supplementary Table 1). In case a significant effect was found ( $P < 0.05$ ), the influence of simulated OA was quantified by computing the effect size. This procedure was identical to the estimation of effect sizes for C/N of organic-matter export, that is, computing the log-transformed response ratio ln(RR) for the CO<sub>2</sub>-treated (OA) versus the control mesocosms. Effect sizes for OA impacts on the various plankton taxa are visualized in the heatmap in Fig. 3a. Note that for the purpose of this visualization, we also included trends with a higher significance threshold ( $P < 0.1$ ). The reason is the relatively low number of observations (mesocosms), for which one outlier can influence the calculated  $P$  value dramatically. Since some detected effect sizes were quite strong, but displayed  $P$  values slightly  $> 0.05$ , we decided to include these effect sizes in the heatmap to avoid (potential) type II errors, that is, overlooking real and possibly large effects due to small sample size. For ease of differentiation, significant  $P$  values ( $< 0.05$ ) are visually marked in Fig. 3.

**Assessing the influence of plankton communities on C/N of organic-matter export.** To explore how different taxonomic and functional groups within the plankton community may have controlled C/N ratios of organic-matter export, we performed linear (Pearson) correlation analysis using biomass from individual plankton taxa and C/N of sediment-trap material. In general, data processing for this approach was very similar to the regression analysis of  $p_{CO_2}$  effects, that is, using temporally averaged data of each individual mesocosm from the different studies.

Correlations were computed for the different experimental periods defined in Table 1, with one important difference: there is generally a distinct time lag between (1) the production (and consumption) of organic matter in the water column and (2) the flux of particulate matter export captured by sediment traps. Work by Stange and colleagues<sup>38</sup> found that this temporal mismatch can

**Table 1 | Overview of distinct experimental phases that were used for analyses of mesocosm data (see Methods and Supplementary Table 1 for details)**

Location	Biome	Experimental phases based on seasonal cycle/succession stage
Svalbard	Arctic	Nutrient-limited: early-summer post-bloom Bloom: induced by nutrient fertilization
Norway	Temperate	Bloom: late-spring bloom and subsequent nutrient fertilization
Finland	Temperate	Nutrient-limited: summer stratification with oligotrophic conditions
Sweden	Temperate	Bloom: spring bloom (diatom-dominated) Nutrient-limited: post-bloom, increased grazing
Gran Canaria	Subtropical	Nutrient-limited: oligotrophic study region Bloom: diatom bloom after simulated upwelling

substantially compromise interpretations of the linkages between water-column processes and export flux. Therefore, we accounted for this temporal lag by using different time windows for water-column data (biomass of plankton groups) and sediment-trap data (C/N of organic-matter export). On the basis of the comparison of bloom peaks and export flux pulses, the time lag identified by Stange et al. differed considerably across studies, ranging from 2 to 15 days for the different mesocosm studies<sup>38</sup>. Accordingly, we used these estimates to adjust the time windows of data on which the correlation analysis for the different experiments is based (Svalbard: 7–8 days; Norway: 4–5 days; Sweden: 4–6 days; Gran Canaria bloom: 10–12 days).

There were, however, two cases for which no numbers of the time lag were available as no distinct bloom peaks and export pulses occurred: the Finland experiment and the first phase of the Gran Canaria study. For these oligotrophic periods, we defined a relatively short time lag of 4 days on the basis of considerations about the ecological drivers behind the time lag. Stange et al. concluded that the time lag between biomass production and export is mainly determined by the degree of coupling between primary producers and grazers<sup>38</sup>. Thus, a strong disequilibrium between production and consumption delays repackaging of phytoplankton biomass into faecal pellets by grazers and thereby one of the major pathways of organic-matter export. On the basis of these considerations, we assumed a tight production–grazing coupling for oligotrophic periods (that is, the entire Finland experiment and the first phase of the Gran Canaria study) and applied a time lag of 4 days, which is at the lower end of the estimates given by Stange and colleagues<sup>38</sup>. In case of the Finland study, this assumption is also supported by stable isotope analysis. Dissolved <sup>15</sup>N was added to the mesocosms as a tracer, and it took about 4–5 days until the signal propagated from suspended organic matter to the sediment-trap material (A. Paul, personal communication).

Obviously, accounting for this time lag constitutes another assumption in our data analysis. However, a direct quantitative comparison of water-column and sediment-trap data from the same period (that is, no time lag) can definitely be considered as inaccurate. For example, the bloom in the Gran Canaria study occurred between days 25 and 35, but the period of high export flux from this bloom was between days 35 and 45. This illustrates that incorporating the time lag into the analysis definitely improves the comparability of water-column processes and export fluxes.

Computed correlation coefficients are visualized in the heatmap in Fig. 3b. Note that for the purpose of this visualization, we also included trends with a higher significance threshold ( $P < 0.1$ ) due to the same reasons as outlined for  $p_{CO_2}$  effect sizes. Furthermore, the visualization of the potential influence of plankton communities on C/N of organic-matter export includes the relative biomass of each plankton taxon as another layer of information. The idea behind this is that taxa with a larger biomass can be expected to have a higher potential of exerting a noticeable imprint on the C/N of particulate organic material, that is, in the course of production by autotrophs as well as via consumption and degradation by heterotrophs.

**Reporting Summary.** Further information on research design is available in the Nature Research Reporting Summary linked to this article.

## Data availability

The raw data of the mesocosm studies are archived in the World Data Centre MARE/PANGAEA ([www.pangaea.de](http://www.pangaea.de)) and can be found using the keyword 'KOSMOS'. In addition, the data supporting the findings of this study are available from the corresponding author upon reasonable request.

## References

30. Boxhammer, T., Bach, L. T., Czerny, J. & Riebesell, U. Technical note: sampling and processing of mesocosm sediment trap material for quantitative biogeochemical analysis. *Biogeosciences* **13**, 2849–2858 (2016).
31. Sharp, J. H. Improved analysis for “particulate” organic carbon and nitrogen from seawater. *Limnol. Oceanogr.* **19**, 984–989 (1974).
32. IPCC *Climate Change 2013: The Physical Science Basis* (eds Stocker, T. F. et al.) (Cambridge Univ. Press, 2013).
33. Hedges, L. V., Gurevitch, J. & Curtis, P. S. The meta-analysis of response ratios in experimental ecology. *Ecology* **80**, 1150–1156 (1999).
34. Schartau, M., Landry, M. R. & Armstrong, R. A. Density estimation of plankton size spectra: a reanalysis of IronEx II data. *J. Plankton Res.* **32**, 1167–1184 (2010).
35. Mackey, M. D., Mackey, D. J., Higgins, H. W. & Wright, S. W. CHEMTAX—a program for estimating class abundances from chemical markers: application to HPLC measurements of phytoplankton. *Mar. Ecol. Prog. Ser.* **144**, 265–283 (1996).
36. Utermöhl, V. H. Neue Wege in der quantitativen Erfassung des Planktons. (Mit besondere Berücksichtigung des Ultraplanktons). *Verh. Internat. Verein. Theor. Angew. Limnol.* **5**, 567–595 (1931).
37. Bach, L. T., Riebesell, U. & Schulz, K. G. Distinguishing between the effects of ocean acidification and ocean carbonation in the coccolithophore *Emiliania huxleyi*. *Limnol. Oceanogr.* **56**, 2040–2050 (2011).
38. Stange et al. Quantifying the time lag between organic matter production and export in the surface ocean: implications for estimates of export efficiency. *Geophys. Res. Lett.* **44**, 268–276 (2017).

## Acknowledgements

This study was supported by the German Federal Ministry of Science and Education (BMBF) in the framework of the projects BIOACID III (Biological Impacts of Ocean Acidification, FKZ 03F0728) and SOPRAN III (Surface Ocean Processes in the

Anthropocene, FKZ 03F0662). Funding for the different mesocosm studies was also provided by the European Project on Ocean Acidification (EPOCA, grant no. 211384) from the European Community’s Seventh Framework Programme (FP7/2007–2013), the EU project MESOAQUA (grant no. 228224), as well as BIOACID II (FKZ 03F06550) and SOPRAN II (03F0611). Furthermore, we thank all participating scientists and technicians for their huge effort in realizing the different studies. We also thank the staff of the marine biological stations in the different study locations for providing logistics, technical assistance and support at all times. We also thank the captains and crews of R/V *Viking Explorer*, M/V *Esperanza* of Greenpeace, R/V *Håkon Mosby* (2011609), R/V *Alkor* (AL376, AL394, AL397, AL406, AL420), R/V *Heincke* (HE360), R/V *Poseidon* (POS463) and R/V *Hesperides* (29HE20140924) for support during transport, deployment and recovery of the mesocosm facilities.

## Author contributions

J.T., L.T.B. and M.S. conceived and designed the meta-analysis. J.T., T.B., P.S., L.T.B., A.J.P. and U.R. coordinated and implemented the mesocosm experiments, including data acquisition. J.T. was responsible for data analysis, data processing and visualization. J.T. wrote the manuscript, with editing by all co-authors.

## Competing interests

The authors declare no competing interests.

## Additional information

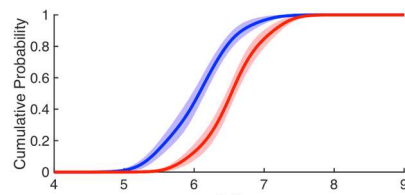
**Extended data** is available for this paper at <https://doi.org/10.1038/s41558-020-00915-5>.

**Supplementary information** is available for this paper at <https://doi.org/10.1038/s41558-020-00915-5>.

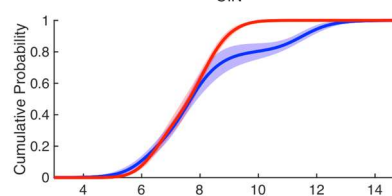
**Correspondence and requests for materials** should be addressed to J.T.

**Reprints and permissions information** is available at [www.nature.com/reprints](http://www.nature.com/reprints).

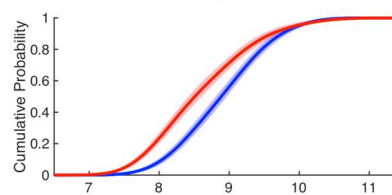
**Svalbard, nutrient-limited**  
(Arctic)



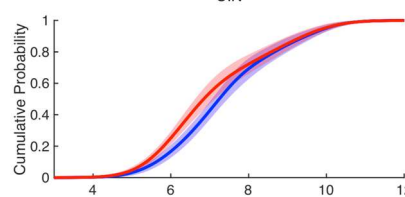
**Svalbard, bloom**  
(Arctic)



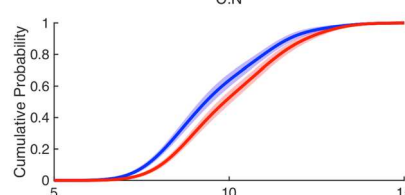
**Norway, bloom**  
(Temperate)



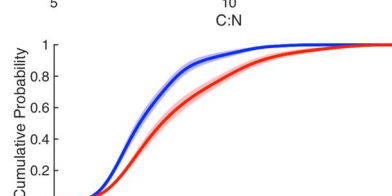
**Finland, nutrient-limited**  
(Temperate)



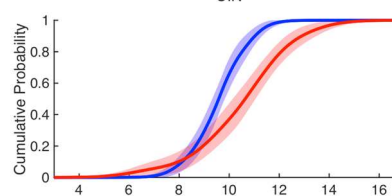
**Sweden, bloom**  
(Temperate)



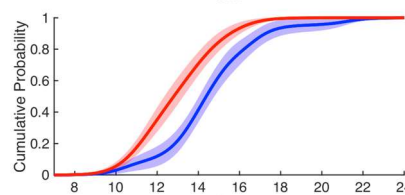
**Sweden, nutrient-limited**  
(Temperate)



**Gran Canaria, nutrient-limited**  
(Subtropical)



**Gran Canaria, bloom**  
(Subtropical)



Ambient – Ocean Acidification

Extended Data Fig. 1 | See next page for caption.

**Extended Data Fig. 1 | Impact of elevated CO<sub>2</sub> concentrations on cumulative probability distributions of C:N<sub>export</sub>.** Shown are ambient conditions (blue) and ocean acidification (red) with shaded areas denoting standard deviation. Data used for analysis is identical with that in Fig. 2, but computed as cumulative values, thereby depicting the visual representation of a Kolmogorov-Smirnov test. Non-overlapping probability distributions indicate statistically significant differences in C:N between ambient and OA conditions. Note different scaling of x-axes due to large variations in baseline C:N among study regions.